



Published in final edited form as:

*Mol Cell Endocrinol.* 2018 October 15; 474: 48–56. doi:10.1016/j.mce.2018.02.006.

## Fat-specific protein 27 is a novel target gene of liver X receptor $\alpha$

Daisuke Aibara<sup>a,1</sup>, Kimihiko Matsusue<sup>a,\*</sup>, Soichi Takiguchi<sup>b</sup>, Frank J. Gonzalez<sup>c</sup>, and Shigeru Yamano<sup>a</sup>

<sup>a</sup>Faculty of Pharmaceutical Science, Fukuoka University, 8–19–1 Nanakuma, Jonan-ku, Fukuoka 814–0180, Japan

<sup>b</sup>Institute for Clinical Research, National Kyushu Cancer Center, 3–1–1 Notame, Minami-ku, Fukuoka 811–1395, Japan

<sup>c</sup>Laboratory of Metabolism, National Cancer Institute, National Institutes of Health, Bethesda, MD 20892, USA

### Abstract

Fat-specific protein 27 (FSP27) is highly expressed in the fatty liver of genetically obese *ob/ob* mice and promotes hepatic triglyceride (TG) accumulation. The nuclear hormone receptor liver X receptor  $\alpha$  (LXR $\alpha$ ) also plays a critical role in the control of TG levels in the liver. The present study demonstrated transcriptional regulation of *Fsp27a* and *Fsp27b* genes by LXR $\alpha$ . Treatment with the LXR ligand T0901317 markedly increased *Fsp27a* and *Fsp27b* mRNAs in wild-type C57BL/6J and *ob/ob* mouse livers. A reporter assay indicated that two LXR-responsive elements (LXREs) are necessary for LXR $\alpha$ -dependent induction of *Fsp27a* and *Fsp27b* promoter activities. Furthermore, the LXR $\alpha$ /retinoid X receptor  $\alpha$  complex is capable of directly binding to the two LXREs both *in vitro* and *in vivo*. These results suggest that LXR $\alpha$  positively regulates *Fsp27a* and *Fsp27b* expression through two functional LXREs. *Fsp27a/b* are novel LXR target genes in the *ob/ob* fatty liver.

### Keywords

PPAR; LXR; Fatty liver; Nuclear receptor

## 1. Introduction

Fat-specific protein 27 (FSP27) was initially isolated by a differential screening approach using mouse adipocyte TA cell lines expressing a mature adipocyte-specific gene (Williams et al., 1992; Danesch et al., 1992). FSP27 belongs to the cell death-inducing DNA fragmentation factor 45-like effector (CIDE) family, which consists of three proteins: CIDEA, CIDEB, and FSP27. The human homolog of mouse FSP27 was also reported as CIDEA (Liang et al., 2003). FSP27 was found to be highly expressed in white and brown adipose tissue and localized to lipid droplets (LDs) in adipocytes (Puri et al., 2007). FSP27 promotes the formation of LD–LD fusions on adipocytes (Gong et al., 2011; Jambunathan et

\*Corresponding author. matsusuk@fukuoka-u.ac.jp (K. Matsusue).

<sup>1</sup>These authors contributed equally to this work.

al., 2011) and enlarged unilocular LDs in cooperation with perilipin 1, another LD-associated protein (Sun et al., 2013). *Fsp27*-null mice showed protection from diet-induced obesity and insulin resistance, and exhibited a small mass of white adipose tissue and the presence of multilocular LDs (Toh et al., 2008; Nishino et al., 2008). Adipocyte-specific *Fsp27*-null mice also exhibited small white adipose tissue masses and hepatic steatosis (Tanaka et al., 2015).

Previous studies demonstrated that hepatic peroxisome proliferator-activated receptor  $\gamma$  (PPAR $\gamma$ ) promoted triglyceride (TG) accumulation and fatty liver development in *ob/ob* mice, a well-characterized model of type 2 diabetes, obesity, and fatty liver because of its mutated *leptin* gene (Matsusue et al., 2003). Furthermore, FSP27 was established as the direct mediator of PPAR $\gamma$ -dependent hepatic steatosis in *ob/ob* mice. Interestingly, FSP27 expression showed the highest levels in *ob/ob* fatty liver, but lower levels in normal liver and led to an increase in hepatic TG levels (Matsusue et al., 2008). Recently, FSP27 isoforms were identified as FSP27 $\alpha$  and FSP27 $\beta$ . FSP27 $\beta$  contains an additional 10 amino acids at the N-terminus of the original FSP27 identified in *ob/ob* fatty liver (named as FSP27 $\alpha$ ) and shows higher intracellular stability than FSP27 $\alpha$ . It was also demonstrated that both isoforms directly promote hepatic TG accumulation (Xu et al., 2015).

Liver X receptor (LXR)  $\alpha$  and  $\beta$  are members of a family of ligand-dependent nuclear receptors (Mangelsdorf et al., 1995). LXRs heterodimerize with retinoid X receptors (RXR) and regulate transcription by binding to LXR-responsive elements (LXRE) of target genes. LXRs play important roles in regulating genes associated with lipogenesis in the liver (Baranowski, 2008). Indeed, activation of LXRs by the LXR ligand, T0901317, caused a marked increase in hepatic TG levels and aggravation of fatty liver in *ob/ob* or other fatty liver model mice (Matsusue et al., 2014; Chisholm and Chisholm, 2003). Regarding hepatic fat accumulation, two transcription factors, sterol regulatory element-binding protein 1c (SREBP1c) and carbohydrate response element-binding protein (ChREBP), play crucial roles in LXR-mediated hepatic lipogenesis (Baranowski, 2008; Matsusue et al., 2014). SREBP1c and ChREBP are direct targets of LXRs and control the expression of nearly all genes integral to lipogenesis, including fatty acid synthase (*Fas*), acetyl-CoA carboxylase, and stearoyl-CoA desaturase 1 (*Scd1*) (Baranowski, 2008; Matsusue et al., 2014). Thus, LXR signaling mediated by SREBP1c and ChREBP is thought to contribute to an increase in hepatic TG content by upregulating these lipogenic genes. Whether LXRs induce not only lipogenic genes but also *Fsp27a/b* in *ob/ob* fatty liver is unknown. Additionally, the transcriptional regulation of hepatic *Fsp27a/b* by LXRs remains unclear.

In the present study, administration of T0901317 to C57BL/6J mice wild-type for the *leptin* gene (*OB/OB*) and *ob/ob* mice showed markedly increased *Fsp27a* and *Fsp27b* expression. Furthermore, two functional LXREs were identified within 5'-upstream regions of *Fsp27a* and *Fsp27b*. These findings suggest that *Fsp27a* and *Fsp27b* are directly regulated by LXR $\alpha$  and a novel LXR $\alpha$  target gene in the liver.

## 2. Materials and methods

### 2.1. Animals and treatment

All animal protocols and studies were performed according to guidelines from the Center for Experimental Animals at Fukuoka University. Eight-week-old male mice (n = 4) on an *ob/ob* background or C57BL/6J mice with a wild-type *leptin* gene (*OB/OB*) were fed an ad *libitum* diet (MF, Oriental Yeast, Fukuoka, Japan) with or without 0.025% (w/w) T0901317 (Sigma Aldrich, St. Louis, MO, USA) for 2 weeks, as previously described (Matsusue et al., 2014). GW3965 (Selleck, Japan) was administered with 20 mg/day/kg for 3 days by oral gavage (Laffitte et al., 2003). As a positive control for oral gavage administration, T0901317 was administered at 20 mg/day/kg for 3 days (Jakel et al., 2004). Vehicle alone was administered as a negative control (0.5% methyl-cellulose).

### 2.2. Total RNA isolation and qPCR

RNA was extracted using TRIzol reagent (Thermo Fisher Scientific, Waltham, MA, USA), and quantitative polymerase chain reaction (qPCR) was performed using cDNA generated from 1 µg of total RNA with an AffinityScript qPCR cDNA Synthesis kit (Agilent Technologies, Santa Clara, CA, USA). The primer sequences used were described previously for the following genes: *Fsp27a* and *Fsp27b*, (Xu et al., 2015); *Lxra*, *Srebp1c*, *Fas*, *Scd1*, *Gpat*, and *Pparg* (Matsusue et al., 2014).

### 2.3. Cell culture

HEK293FT cells were cultured at 37 °C under 5% CO<sub>2</sub> in Dulbecco's Modified Eagle's Medium with high glucose and pyruvate (Thermo Fisher Scientific), supplemented with 10% fetal bovine serum (Biowest, Nuaille, France) and 1% Antibiotic-Antimycotic (Thermo Fisher Scientific).

### 2.4. Construction of reporter and expression plasmids

The transcriptional start sites of mouse *Fsp27a* and *Fsp27b* were determined previously (Danesch et al., 1992; Xu et al., 2015). The -1698 (A1), -1426 (A2), -1267 (A3), and -139 (A4) base pair (bp) fragments from the transcriptional start site (+1) of the mouse *Fsp27a* 5'-upstream region, containing KpnI and MluI sites at the 5'- and 3'-end of the primers, were amplified by PCR and cloned into the luciferase reporter vector pGL3 basic (Promega, Madison, WI, USA) as previously described (Matsusue et al., 2008).

Internal deletion constructs for *Fsp27a* were prepared by inverse PCR. The *Fsp27a* A4 construct was used as a template. The primer sequences were as follows: A4-1 forward, 5'-GGAGCTGGGGTATATGGC-3' and reverse, 5'-CCCAGCCTCCTGGCAATA-3'; A4-2 forward, 5'-ATGGCTGAGGTCGCAGTT-3' and reverse, 5'-CCATGTCCTTATATACC-3'; A4-3 forward, 5'-ATAAGGGACATGGTTGGA-3' and reverse, 5'-ATATACCCCAGCTCCTCA-3'.

The -2647 (B1), -2375 (B2), -1382 (B3), and -806 (B4) bp fragments from the transcriptional start site (+1) of the mouse *Fsp27b* 5'-upstream region, containing CACC sites at the 5'-end of the primers, were amplified by PCR and cloned into the Gateway entry

vector pENTR/D-TOPO (Thermo Fisher Scientific), and then recombined into the destination vector pGL4.17 (Promega), which was prepared using the Gateway Vector Conversion System according to the manufacturer's instructions (Thermo Fisher Scientific). The primer sequences were as follows: B1 forward, 5'-CACCTCCCATTGCTCATTCG-3'; B2 forward, 5'-CACCATCAGCTGTGCCTACGGATG-3'; B3 forward, 5'-CACCTGAGACAGGGCCAACCTCT-3'; B4 forward, 5'-CACCAGTGTGGGTTGTGGTGAGG-3'; reverse for all constructs, 5'-TGTTTCTCCGACCCAAGCTG-3'.

The LXR $\alpha$  and RXR $\alpha$  expression vectors were prepared as described previously (Matsusue et al., 2006). The complete open reading frame of mouse LXR $\beta$  was amplified by PCR from a mouse liver cDNA library by using gene-specific primers and cloned into the Gateway entry vector, pENTR/D-TOPO (Thermo Fisher Scientific). This sequence was then recombined into the destination vector, pcDNA3.1 (Thermo Fisher Scientific), which was prepared using the Gateway Vector Conversion System (Thermo Fisher Scientific). The primer sequences were as follows: forward, 5'-CACCACCATGGCTTCCCCACAAGTTCTCTGG-3' and reverse, 5'-CATCTTCAAGAAGACACCACCAAG-3'.

## 2.5. Transient transfection and reporter assay

HEK293FT cells were seeded at a density of  $2.0 \times 10^5$  cells/well in 24-well plates at 24 h prior to transfection. Cells were transfected with plasmids using jetPEI DNA transfection reagent (Polyplus-transfection, Illkirch, France) according to the manufacturer's instructions. Typically, each well contained 2  $\mu$ L of jetPEI DNA transfection reagent, 0.15  $\mu$ g of LXR $\alpha$  (or LXR $\beta$ ) and RXR $\alpha$  expression plasmids, 0.4  $\mu$ g of luciferase reporter constructs containing the 5'-region of mouse *Fsp27a/b*, and 0.05  $\mu$ g of phRL/TK (Promega) as an internal control for transfection efficiency. After adding the reagents, cells were transfected for 6 h at 37 °C in an atmosphere of 5% CO<sub>2</sub>. The cells were then incubated for 42 h in fresh medium containing 10  $\mu$ M T0901317, 10  $\mu$ M GW3965, 0.1  $\mu$ M LG100268 (Sigma-Aldrich), or DMSO. The luciferase assay was performed using the Dual-Luciferase Reporter Assay System (Promega). Luciferase activity was measured using a GENE LIGHT 55A luminometer (Nition, Microtec Co., Ltd., Chiba, Japan).

## 2.6. In vitro transcription/translation and EMSA

Mouse LXR $\alpha$  and human RXR $\alpha$  proteins were synthesized *in vitro* from LXR $\alpha$  and RXR $\alpha$  expression plasmids using the TNT Quick Coupled Transcription/Translation System (Promega) according to the manufacturer's protocols. Electrophoretic mobility shift assay (EMSA) was performed as described previously (Matsusue et al., 2006). For the supershift assay, 0.5  $\mu$ g of anti-LXR $\alpha$  IgG (Perseus Proteomics, Tokyo, Japan) was included for 30 min after the binding reactions. The gels were exposed to an imaging plate. The gel images were visualized using an FLA-7000 imaging analyzer (Fujifilm, Tokyo, Japan). Probe sequences for the EMSA were as follows: mouse phosphofructokinase-2 (*pfk2*) LXRE (Zhao et al., 2012), 5'-CTCTCCTGACCTCTCCCAACCTCTGCGG-3'; non-LXRE, 5'-GCACACACCTTTAGTCCCGGCTCTCTGG-3'; LXRE-1, 5'-

CCGGACAGGTGACTACAGGACAGAAAGG-3'; LXRE-2, 5'-  
CCACGGAGGCCTGACGAGGTGACAGATC-3'; LXRE-3, 5'-  
GGTATATGGCTACTAGAGAGCAGATGGT-3'.

## 2.7. ChIP assay

Chromatin immunoprecipitation (ChIP) assays were performed using a SimpleChIP Enzymatic Chromatin IP Kit-Magnetic Beads (Cell Signaling Technology, Danvers, MA, USA) according to the manufacturer's protocols. Briefly, T0901317-treated *ob/ob* mouse livers were treated with 1% formaldehyde for 10 min. The isolated nuclei were digested with micrococcal nuclease and further sonicated. Anti-LXR $\alpha$  IgG (Perseus Proteomics) was used to immunoprecipitate LXR $\alpha$ -binding DNA fragments. The precipitated chromatin was digested with proteinase K for 2 h at 65 °C. Finally, DNA was purified using a spin column and subjected to qPCR. Primer sequences for ChIP-qPCR were as follows; non-PPRE forward, 5'-CTGACGTGTGGTTAGAGACATGG-3' and reverse, 5'-GTGTATTTGTGCACGTGAGAGC-3'; LXRE-1 forward, 5'-GAAGGAATGTCGCCTCTCCAG-3' and reverse, 5'-CTAAGGCAGCAACACGAAGC-3'; LXRE-3' forward, 5'-GCTGGGGTATATGGCTACTAGAGAG-3' and reverse, 5'-GATTAACGCAGGTTCTCCTTGG-3'.

## 2.8. Statistical analysis

Experimental values are expressed as the mean  $\pm$  standard error of the mean (S.E.M.). Statistical analysis was performed using Student's *t*-test for unpaired data, with  $P < 0.05$  considered to indicate statistical significance.

## 3. Results

### 3.1. *Fsp27a* and *Fsp27b* expression in *OB/OB* and *ob/ob* mouse livers is induced by T0901317

Treatment with T0901317 led to a marked increase in liver weight and hepatic TG levels in *ob/ob* mice (Matsusue et al., 2014). The same effect of the ligand was observed in another obese model, *db/db* mice (Chisholm and Chisholm, 2003). To examine the expression of hepatic *Fsp27a* and *Fsp27b* in LXR-dependent fatty liver, the mRNA of both genes was measured in ligand-treated *OB/OB* and *ob/ob* mice. The expression of *Fsp27a* mRNA in *OB/OB* and *ob/ob* mouse livers was induced by approximately 3.0- and 6.0-fold with T0901317 compared to that in the control (Fig. 1A). Furthermore, the expression of *Fsp27b* mRNA in T0901317-treated *OB/OB* and *ob/ob* mouse livers was 6.0- and 9.0-fold higher than in each control liver (Fig. 1B).

Although the expression of LXR $\alpha$  by T0901317 slightly decreased in *OB/OB* and *ob/ob* livers, the expression of LXR-target genes, *Srebp1c*, *Fas*, *Scd1*, and glycerol-3-phosphate acyltransferase (*Gpat*) mRNAs significantly increased in both livers (Fig. 1C–G). The expression of hepatic PPAR $\gamma$  was induced in *ob/ob* fatty liver (Matsusue et al., 2003) and activated PPAR $\gamma$  induced *Fsp27a* mRNA expression in fatty liver (Matsusue et al., 2008). T0901317 had no significant effect on the expression of hepatic *Pparg* mRNA in *OB/OB* and *ob/ob* livers (Fig. 1H). T0901317 has been reported to activate the farnesoid X receptor

(FXR) or pregnane X receptor (PXR) (Mitro et al., 2007). To evaluate the LXR-specific regulation of *Fsp27a* (Fig. 1I) or *Fsp27b* (Fig. 1J) mRNA, the expression of both genes by an LXR-specific ligand, GW3965, was examined in the *OB/OB* liver. The results revealed that both *Fsp27a* and *Fsp27b* mRNAs were significantly induced approximately 2.0-fold with GW3965 as compared to that in the control. As a positive control for the same oral gavage administration, the expression of *Fsp27a* and *Fsp27b* mRNAs was induced by approximately 5.0- and 4.0-fold with T0901317. These results suggest that LXR $\alpha$  positively regulates *Fsp27a* and *Fsp27b* expression in *OB/OB* and *ob/ob* livers.

### 3.2. Three putative LXREs on 5'-upstream and exon 1 of *Fsp27a* and *Fsp27b*

*Fsp27a* and *Fsp27b* show differences in exon 1, termed as a and b, respectively, while exons 2–6 are the same (Fig. 2A) (Xu et al., 2015). Thus, the promoter regions for *Fsp27a* or *Fsp27b* differ. To detect functional LXRE in the *Fsp27a/b* 5'-upstream region, database analysis was performed. By searching the JASPAR database (<http://jaspar.genereg.net/>), three putative LXREs were identified (Fig. 2A). Interestingly, LXRE-3 of *Fsp27a* was located in a 5'-untranslated region (5'-UTR) of exon 1a. LXRE-1, LXRE-2, and LXRE-3 showed 83%, 75%, and 58% homology with a typical LXRE consensus sequence (Willy et al., 1995), respectively. Human CIDEA as the homolog of mouse FSP27 also contained LXRE at a position corresponding to LXRE-3.

To determine how LXR $\alpha$  regulates the promoter activity of *Fsp27a* and *Fsp27b*, *Fsp27a* (–1698/+257 bp) or *Fsp27b* (–2647/+77 bp), luciferase reporter plasmids containing the three putative LXREs, were constructed. *Fsp27a* or *Fsp27b* reporter and the LXR $\alpha$  and RXR $\alpha$  expression plasmids were transfected into HEK293FT cells. The relative fold-inductions of *Fsp27a* promoter activity with LXR $\alpha$  and RXR $\alpha$ , compared to that without LXR $\alpha$ , were as follows: non-LXR ligand, 3.0-fold; with T0901317, 5.0-fold; and with GW3965, 5.0-fold (Fig. 2Ba). Similarly, the relative fold-inductions of *Fsp27b* activity were as follows: non-LXR ligand, 1.2-fold; with T0901317, 1.5-fold; and with GW3965, 1.5-fold (Fig. 2Bb). The effects of the RXR-specific ligand LG100268 in the presence of LXR $\alpha$ , RXR $\alpha$  and T0901317 or GW3965 showed a similar tendency for *Fsp27a* and *Fsp27b* promoter activities. The relative fold-inductions of *Fsp27a/b* promoter activity with LG100268, compared to without LG100268, were as follows: non-LXR ligand, 1.3-fold; with T0901317, 1.5-fold; and with GW3965, 1.5-fold (Fig. 2Ba and b). Furthermore, the effect of LXR $\beta$  expression on the promoter activity of *Fsp27a* and *Fsp27b* was examined. In the presence of RXR $\alpha$  and T0901317 or GW3965, the *Fsp27a* promoter activity with LXR $\beta$  was induced by approximately 5.5-fold with T0901317 and 6.0-fold with GW3965 compared to that without LXR $\beta$  (Fig. 2Bc). In contrast, *Fsp27b* promoter activity with LXR $\beta$  was induced approximately 1.5-fold with T0901317 and 2.0-fold with GW3965 (Fig. 2Bd).

### 3.3. Identification of a functional LXRE of *Fsp27a* and *Fsp27b*

To identify the *cis*-element responsible for ligand-dependent promotion by LXR $\alpha$ , reporter constructs with serial deletions of the 5'-flanking DNA regions of *Fsp27a* and *Fsp27b* were prepared. The luciferase activity of the *Fsp27a* A1 construct was induced by approximately 7.0-fold with LXR $\alpha$ , whereas the activity of the A2 construct lacking LXRE-1 decreased by

approximately 60% compared to the A1 construct. The activity of the A3 and A4 constructs lacking LXRE-2 was not different from that of the A2 construct (Fig. 3Aa). LXRE-3 is in the 5'-UTR of exon 1a of *Fsp27a* (Fig. 2A). Thus, to determine the role of LXRE-3 in LXR ligand-dependent promotion, an internal deletion mutant of LXRE-3 using the *Fsp27a* A4 construct was prepared. The *Fsp27a* A4 construct including LXRE-3 was induced by approximately 4.5-fold with LXR $\alpha$  (Fig. 3Ab). Although upstream or downstream deletion of LXRE-3 led to a slight decrease in the induction by LXR $\alpha$  (A4-1 or A4-2), the induction was completely lost in the A4-3 construct lacking LXRE-3 (Fig. 3Ab). Furthermore, LXR ligand-dependent promotion of *Fsp27b* also depended on LXRE-1 and LXRE-3. Luciferase activity of the *Fsp27b* B1 construct was induced by approximately 2.5-fold with LXR $\alpha$ , whereas the activity of the B2 construct lacking LXRE-1 decreased by approximately 60%. This induction was nearly lost in the B4 construct lacking LXRE-3 (Fig. 3B). These results suggest that LXR $\alpha$  induces the promoter activity of *Fsp27a* and *Fsp27b* through LXRE-1 and LXRE-3.

#### 3.4. LXR $\alpha$ /RXR $\alpha$ heterodimer directly binds to LXRE-1 and LXRE-3

To examine whether LXR $\alpha$  directly binds to LXRE-1 and LXRE-3, electrophoretic mobility shift assays using LXRE probes for *Fsp27a* and *Fsp27b*, with *Pfk2* as a positive control probe (Zhao et al., 2012), were performed. Although LXR $\alpha$  or RXR $\alpha$  did not bind to all LXRE probes, the LXR $\alpha$ /RXR $\alpha$  heterodimer directly bound to control-LXRE, LXRE-1, and LXRE-3, but not LXRE-2 (Fig. 4A) *in vitro*. The binding of LXR $\alpha$ /RXR $\alpha$  to LXRE-1 and LXRE-3 was nearly lost by adding a 200-fold molar excess of each unlabeled probe. Furthermore, the binding of LXR $\alpha$ /RXR $\alpha$  to LXRE-1 and LXRE-3 were supershifted by the addition of anti-LXR $\alpha$  IgG (Fig. 4B). These results suggest that LXR $\alpha$ /RXR $\alpha$  heterodimers directly bind to LXRE-1 and LXRE-3 of *Fsp27a* and *Fsp27b*.

#### 3.5. Endogenous LXR $\alpha$ in *ob/ob* fatty liver interacts with LXRE-1 and LXRE-3

To examine the interactions between endogenous LXR $\alpha$  and LXRE-1 or LXRE-3 under physiological conditions, a ChIP assay was performed with chromatin from T0901317-treated *ob/ob* mouse liver. Three primer sets were designed to amplify LXRE-1, LXRE-3, and non-LXRE (negative control) (Fig. 5A). The chromatin from cross-linked liver was fragmented and incubated with anti-LXR $\alpha$  IgG (LXR $\alpha$ ) or anti-rabbit IgG (Control) as a negative control. Precipitated LXREs were detected by qPCR using each ChIP primer. The results revealed an association of endogenous LXR $\alpha$  in *ob/ob* fatty liver with LXRE-1 and LXRE-3. The addition of anti-LXR $\alpha$  IgG led to an increase of approximately 2.0-fold in LXRE-1 and LXRE-3 as compared to the control IgG, although the non-LXRE signal slightly increased (Fig. 5B). These results suggest that endogenous LXR $\alpha$  also interacts with LXRE-1 and LXRE-3 in *ob/ob* mouse fatty liver.

## 4. Discussion

The present study demonstrated a novel regulation mechanism of *Fsp27a* and *Fsp27b* by LXR $\alpha$ . An LXR $\alpha$  ligand, T0901317, markedly increased *Fsp27a* and *Fsp27b* mRNAs in *OB/OB* and *ob/ob* mouse livers. *Fsp27a* and *Fsp27b* contain two functional LXREs, LXRE-1 and LXRE-3. LXR $\alpha$  directly binds to these LXREs *in vitro* and *in vivo*.

Interestingly, LXRE-3 of *Fsp27a* is located in the 5'-UTR of exon 1a, which is also observed for the LXREs of the *ATP-binding cassette transporter 1* (Schwartz et al., 2000) or *organic anion transporting polypeptide 1B1* (Meyer Zu Schwabedissen et al., 2010) genes. The LXR family consists of two members, LXR $\alpha$  and LXR $\beta$ , which are encoded by individual genes (Alberti et al., 2000). Mouse LXR $\alpha$  is highly expressed in the liver and kidney, while LXR $\beta$  is ubiquitously expressed (Seol et al., 1995). The present study revealed induction of *Fsp27a* and *Fsp27b* promoter activities by LXR $\beta$ . Therefore, LXR $\beta$  also appears to contribute to regulating hepatic *Fsp27a* and *Fsp27b*.

T0901317 potentially activates not only LXRs, but also FXR or PXR (Houck et al., 2004). Thus, the involvement of T0901317-activated FXR or others in regulating hepatic *Fsp27a* and *Fsp27b* cannot be ruled out. However, *Fxr*-null mice exhibited elevated hepatic TG levels as opposed to the phenotype displayed by *Lxr*-null mice (Sinal et al., 2000; Beaven et al., 2013). Another study found no significant difference in the expression of *Fsp27a* mRNA in white adipose tissue between wild-type and *Fxr*-null mice (Abdelkarim et al., 2010). Thus, FXR likely does not or only slightly contributes to regulating *Fsp27a* and *Fsp27b* in the liver. Notably, the LXR-specific ligand GW3965 significantly induced *Fsp27a* or *Fsp27b* mRNA in the *OB/OB* liver. These results support that LXR $\alpha/\beta$  positively regulates the transcriptional expression of *Fsp27a* or *Fsp27b* in the liver.

It has reported that *Lxra* mRNA in human macrophages or mouse adipose tissue is induced by T0901317-activated LXR through LXRE located in the 5'-upstream region (Whitney et al., 2001; Ulven et al., 2004). However, we found that *Lxra* mRNA was slightly decreased by T0901317 administration. The discrepancy may be related to the tissue or cell-specific manner of self-regulation of LXR $\alpha$  by LXR (Whitney et al., 2001; Ulven et al., 2004), although the mechanism of the specificity remains unclear. Indeed, a study showed that the levels of hepatic *Lxra* mRNA in T0901317-administered mice were lower than in untreated mice, which agrees with our results (Matusue et al., 2014; Ulven et al., 2004). Further, we examined whether *Lxra* protein levels between control and T0901317-treated livers remain unchanged (data not shown).

The fatty liver of *ob/ob* mice was found to result from PPAR $\gamma$  induction of FSP27 through a typical PPRE in the *Fsp27* promoter region (Matusue et al., 2008). It was reported that *Fsp27* mRNA is upregulated by PPAR $\alpha$  (Langhi and Baldan, 2015) or cAMP-response element-binding protein (Vila-Brau et al., 2013) in *OB/OB* livers. In these earlier reports, *Fsp27* mRNA was not distinguished between *Fsp27a* and *Fsp27b* mRNAs and was used as the primer set for the common exon sequence in *Fsp27a/b*. Additionally, cyclic AMP-responsive element-binding protein H (CREBH) was also reported as a critical factor for *Fsp27b* mRNA induction in the fasting normal liver or *ob/ob* fatty liver (Xu et al., 2015). Interestingly, induction by CREBH occurred in an *Fsp27b*-specific manner because the CREBH response element is located in the promoter region of *Fsp27b*. In contrast to CREBH, activated LXR $\alpha$  upregulates both *Fsp27a* and *Fsp27b* in fatty liver and upregulates hepatic lipogenesis by controlling lipogenic genes. Because the expression of all LXR targets without T0901317 in the *ob/ob* fatty liver was higher than that in the normal liver, LXRs appear to be constitutively active in the fatty liver. The hepatic TG levels increased by activated LXRs are thought to be accompanied by elevated SREBP1c, ACC, FAS, and SCD1



(Baranowski, 2008). Notably, FSP27 $\alpha$  and FSP27 $\beta$  may promote hepatic TG accumulation (Matsusue et al., 2008; Xu et al., 2015). Therefore, LXRs likely promote not only TG synthesis by lipogenic enzymes, but also TG accumulation through FSP27 $\alpha$  and FSP27 $\beta$ . TG synthesis and accumulation by LXRs appear to largely contribute to the development and aggregation of fatty liver.

In summary, the present study demonstrated that hepatic *Fsp27a* and *Fsp27b* are positively regulated by LXR $\alpha$  through two functional LXREs. CIDEc, the human homolog of mouse *Fsp27*, also has an LXRE in the 5'-upstream region. Therefore, elucidating the mechanism of TG-accumulating effects by LXRs through FSP27 $\alpha$  and FSP27 $\beta$  may lead to new therapeutic opportunities for controlling TG accumulation in non-alcoholic fatty liver disease and its associated pathologies.

## Acknowledgments

### Funding

This work was supported by a Grant from KAKENHI (17K08799) and funds (No. 147015) from the Central Research Institute of Fukuoka University.

## Abbreviations:

<b>FSP27</b>	fat-specific protein 27
<b>CIDE</b>	cell death-inducing DNA fragmentation factor 45-like effector
<b>LD</b>	lipid droplet
<b>TG</b>	triglyceride
<b>PPAR</b>	peroxisome proliferator-activated receptor
<b>CREBH</b>	cyclic AMP-responsive element binding protein H
<b>LXR</b>	liver X receptor
<b>LXRE</b>	LXR response element
<b>FAS</b>	fatty acid synthase
<b>SCD1</b>	stearoyl-coenzyme A desaturase 1
<b>PFK2</b>	phosphofructokinase-2
<b>SREBP1c</b>	sterol regulatory element-binding protein-1c
<b>ChREBP</b>	carbohydrate response element-binding protein
<b>ACC</b>	acetyl CoA carboxylase
<b>GPAT</b>	glycerol-3-phosphate acyltransferase
<b>UTR</b>	untranslated region

<b>ob/ob</b>	leptin-deficient mice
<b>OB/OB</b>	C57BL/6J wild-type for leptin gene

## References

- Abdelkarim M, Caron S, Duhem C, Prawitt J, Dumont J, Lucas A, Bouchaert E, Briand O, Brozek J, Kuipers F, Fievet C, Cariou B, Staels B, 2010 The farnesoid X receptor regulates adipocyte differentiation and function by promoting peroxisome proliferator-activated receptor-gamma and interfering with the Wnt/beta-catenin pathways. *J. Biol. Chem* 285, 36759–36767. [PubMed: 20851881]
- Alberti S, Steffensen KR, Gustafsson JA, 2000 Structural characterisation of the mouse nuclear oxysterol receptor genes LXRalpha and LXRbeta. *Gene* 243, 93–103. [PubMed: 10675617]
- Baranowski M, 2008 Biological role of liver X receptors. *J. Physiol. Pharmacol* 59 (Suppl 7), 31–55. [PubMed: 19258656]
- Beaven SW, Matveyenko A, Wroblewski K, Chao L, Wilpitz D, Hsu TW, Lentz J, Drew B, Hevener AL, Tontonoz P, 2013 Reciprocal regulation of hepatic and adipose lipogenesis by liver X receptors in obesity and insulin resistance. *Cell Metabol.* 18, 106–117.
- Chisholm JW, Chisholm JW, 2003 The LXR ligand T0901317 induces severe lipogenesis in the db/db diabetic mouse. *J. Lipid Res* 44, 2039–2048. [PubMed: 12923232]
- Danesch U, Hoeck W, Ringold GM, 1992 Cloning and transcriptional regulation of a novel adipocyte-specific gene, FSP27. CAAT-enhancer-binding protein (C/EBP) and C/EBP-like proteins interact with sequences required for differentiation-dependent expression. *J. Biol. Chem* 267, 7185–7193. [PubMed: 1339452]
- Gong J, Sun Z, Wu L, Xu W, Schieber N, Xu D, Shui G, Yang H, Parton RG, Li P, 2011 Fsp27 promotes lipid droplet growth by lipid exchange and transfer at lipid droplet contact sites. *J. Cell Biol* 195, 953–963. [PubMed: 22144693]
- Houck KA, Borchert KM, Hepler CD, Thomas JS, 2004 T0901317 is a dual LXR/FXR agonist. *Mol. Genet. Metabol.* 83, 184–187.
- Jakel H, Nowak M, Moitrot E, Dehondt H, Hum DW, Pennacchio LA, Fruchart-Najib J, Fruchart J-C, 2004 The liver X receptor ligand T0901317 down-regulates APOA5 gene expression through activation of SREBP-1c. *J. Biol. Chem* 279, 45462–45469. [PubMed: 15317819]
- Jambunathan S, Yin J, Khan W, Tamori Y, Puri V, 2011 FSP27 promotes lipid droplet clustering and then fusion to regulate triglyceride accumulation. *PLoS One* 6, e28614. [PubMed: 22194867]
- Laffitte BA, Chao LC, Li J, Walczak R, Hummasti S, Joseph SB, Castrillo A, Wilpitz DC, Mangelsdorf DJ, Collins JL, Saez E, Tontonoz P, 2003 Activation of liver X receptor improves glucose tolerance through coordinate regulation of glucose metabolism in liver and adipose tissue. *Proc. Natl. Acad. Sci. U.S.A* 100, 5419–5424. [PubMed: 12697904]
- Langhi C, Baldan A, 2015 CIDEC/FSP27 is regulated by peroxisome proliferator-activated receptor alpha and plays a critical role in fasting- and diet-induced hepatosteatosis. *Hepatology* 61, 1227–1238. [PubMed: 25418138]
- Liang L, Zhao M, Xu Z, Yokoyama KK, Li T, 2003 Molecular cloning and characterization of CIDE-3, a novel member of the cell-death-inducing DNA-fragmentation-factor (DFF45)-like effector family. *Biochem. J* 370, 195–203. [PubMed: 12429024]
- Mangelsdorf DJ, Thummel C, Beato M, Herrlich P, Schutz G, Umesono K, Blumberg B, Kastner P, Mark M, Chambon P, Evans RM, 1995 The nuclear receptor superfamily: the second decade. *Cell* 83, 835–839. [PubMed: 8521507]
- Matsusue K, Haluzik M, Lambert G, Yim SH, Gavrilova O, Ward JM, Brewer B Jr., Reitman ML, Gonzalez FJ, 2003 Liver-specific disruption of PPARgamma in leptin-deficient mice improves fatty liver but aggravates diabetic phenotypes. *J. Clin. Invest* 111, 737–747. [PubMed: 12618528]
- Matsusue K, Miyoshi A, Yamano S, Gonzalez FJ, 2006 Ligand-activated PPAR-beta efficiently represses the induction of LXR-dependent promoter activity through competition with RXR. *Mol. Cell. Endocrinol.* 256, 23–33. [PubMed: 16806672]

- Matsusue K, Kusakabe T, Noguchi T, Takiguchi S, Suzuki T, Yamano S, Gonzalez FJ, 2008 Hepatic steatosis in leptin-deficient mice is promoted by the PPAR $\gamma$  target gene Fsp27. *Cell Metabol.* 7, 302–311.
- Matsusue K, Aibara D, Hayafuchi R, Matsuo K, Takiguchi S, Gonzalez FJ, Yamano S, 2014 Hepatic PPAR $\gamma$  and LXR $\alpha$  independently regulate lipid accumulation in the livers of genetically obese mice. *FEBS Lett.* 588, 2277–2281. [PubMed: 24857376]
- Meyer Zu Schwabedissen HE, Bottcher K, Chaudhry A, Kroemer HK, Schuetz EG, Kim RB, 2010 Liver X receptor alpha and farnesoid X receptor are major transcriptional regulators of OATP1B1. *Hepatology* 52, 1797–1807. [PubMed: 20827719]
- Mitro N, Vargas L, Romeo R, Koder A, Saez E, 2007 T0901317 is a potent PXR ligand: implications for the biology ascribed to LXR. *FEBS Lett.* 581, 1721–1726. [PubMed: 17418145]
- Nishino N, Tamori Y, Tateya S, Kawaguchi T, Shibakusa T, Mizunoya W, Inoue K, Kitazawa R, Kitazawa S, Matsuki Y, Hiramatsu R, Masubuchi S, Omachi A, Kimura K, Saito M, Amo T, Ohta S, Yamaguchi T, Osumi T, Cheng J, Fujimoto T, Nakao H, Nakao K, Aiba A, Okamura H, Fushiki T, Kasuga M, 2008 FSP27 contributes to efficient energy storage in murine white adipocytes by promoting the formation of unilocular lipid droplets. *J. Clin. Invest* 118, 2808–2821. [PubMed: 18654663]
- Puri V, Konda S, Ranjit S, Aouadi M, Chawla A, Chouinard M, Chakladar A, Czech MP, 2007 Fat-specific protein 27, a novel lipid droplet protein that enhances triglyceride storage. *J. Biol. Chem* 282, 34213–34218. [PubMed: 17884815]
- Schwartz K, Lawn RM, Wade DP, 2000 ABC1 gene expression and ApoA-I-mediated cholesterol efflux are regulated by LXR. *Biochem. Biophys. Res. Commun* 274, 794–802. [PubMed: 10924356]
- Seol W, Choi HS, Moore DD, 1995 Isolation of proteins that interact specifically with the retinoid X receptor: two novel orphan receptors. *Mol. Endocrinol* 9, 72–85. [PubMed: 7760852]
- Sinal CJ, Tohkin M, Miyata M, Ward JM, Lambert G, Gonzalez FJ, 2000 Targeted disruption of the nuclear receptor FXR/BAR impairs bile acid and lipid homeostasis. *Cell* 102, 731–744. [PubMed: 11030617]
- Sun Z, Gong J, Wu H, Xu W, Wu L, Xu D, Gao J, Wu JW, Yang H, Yang M, Li P, 2013 Perilipin1 promotes unilocular lipid droplet formation through the activation of Fsp27 in adipocytes. *Nat. Commun* 4, 1594. [PubMed: 23481402]
- Tanaka N, Takahashi S, Matsubara T, Jiang C, Sakamoto W, Chanturiya T, Teng R, Gavrilova O, Gonzalez FJ, 2015 Adipocyte-specific disruption of fat-specific protein 27 causes hepatosteatosis and insulin resistance in high-fat diet-fed mice. *J. Biol. Chem* 290, 3092–3105. [PubMed: 25477509]
- Toh SY, Gong J, Du G, Li JZ, Yang S, Ye J, Yao H, Zhang Y, Xue B, Li Q, Yang H, Wen Z, Li P, 2008 Up-regulation of mitochondrial activity and acquirement of brown adipose tissue-like property in the white adipose tissue of fsp27 deficient mice. *PLoS One* 3, e2890. [PubMed: 18682832]
- Ulven SM, Dalen KT, Gustafsson J-Å, Nebb HI, 2004 Tissue-specific autoregulation of the LXRalpha gene facilitates induction of apoE in mouse adipose tissue. *J. Lipid Res* 45, 2052–2062. [PubMed: 15292368]
- Vila-Brau A, De Sousa-Coelho AL, Goncalves JF, Haro D, Marrero PF, 2013 Fsp27/CIDEA is a CREB target gene induced during early fasting in liver and regulated by FA oxidation rate. *J. Lipid Res* 54, 592–601. [PubMed: 23220584]
- Whitney KD, Watson MA, Goodwin B, Galardi CM, Maglich JM, Wilson JG, Willson TM, Collins JL, Kliewer SA, 2001 Liver X receptor (LXR) regulation of the LXRalpha gene in human macrophages. *J. Biol. Chem* 276, 43509–43515. [PubMed: 11546778]
- Williams PM, Chang DJ, Danesch U, Ringold GM, Heller RA, 1992 CCAAT/enhancer binding protein expression is rapidly extinguished in TA1 adipocyte cells treated with tumor necrosis factor. *Mol. Endocrinol* 6, 1135–1141. [PubMed: 1508226]
- Willy PJ, Umesono K, Ong ES, Evans RM, Heyman RA, Mangelsdorf DJ, 1995 LXR, a nuclear receptor that defines a distinct retinoid response pathway. *Genes Dev.* 9, 1033–1045. [PubMed: 7744246]

- Xu X, Park JG, So JS, Lee AH, 2015 Transcriptional activation of Fsp27 by the liver-enriched transcription factor CREBH promotes lipid droplet growth and hepatic steatosis. *Hepatology* 61, 857–869. [PubMed: 25125366]
- Zhao LF, Iwasaki Y, Nishiyama M, Taguchi T, Tsugita M, Okazaki M, Nakayama S, Kambayashi M, Fujimoto S, Hashimoto K, Murao K, Terada Y, 2012 Liver X receptor alpha is involved in the transcriptional regulation of the 6-phosphofructo-2-kinase/fructose-2,6-bisphosphatase gene. *Diabetes* 61, 1062–1071. [PubMed: 22415873]

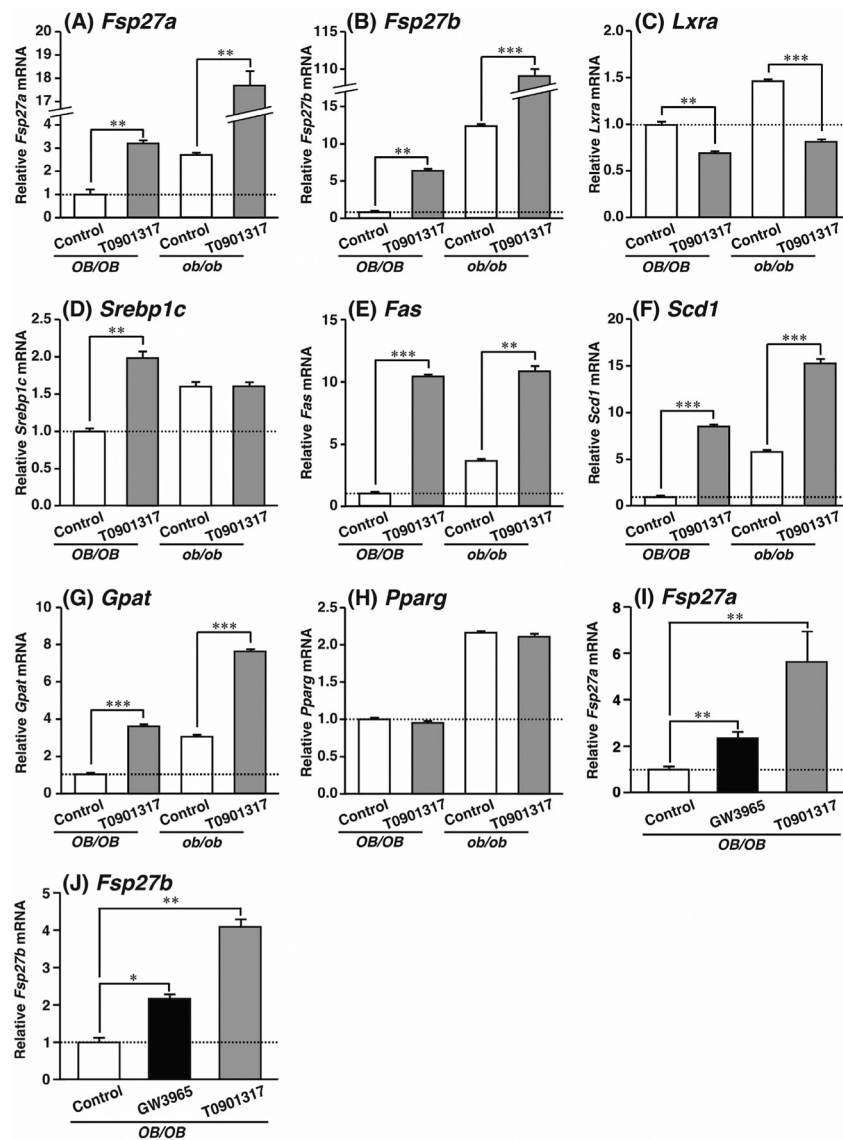


**Fig. 1. T0901317 increases the expression levels of *Fsp27a* and *Fsp27b* in *OB/OB* and *ob/ob* mouse livers.**

T0901317 was administered at 0.025% (w/w) for 2 weeks in ligand-mixed diets. qPCR analyses of (A) *Fsp27a*, (B) *Fsp27b*, (C) *Lxra*, (D) *Srebp1c*, (E) *Fas*, (F) *Scd1*, (G) *Gpat*, and (H) *Pparg* mRNAs were examined using liver samples from T0901317-treated *OB/OB* and *ob/ob* mice. Effect of GW3965 on *Fsp27a* (I) or *Fsp27b* (J) mRNA was examined using liver samples from T0901317- or GW3965-treated *OB/OB* mice. T0901317 or GW3965 was administered at 20 mg/day/kg for 3 days by oral gavage. Gene expression was normalized to *36b4* mRNA. Each bar represents the average  $\pm$  S.E.M. of four individual experiments. *OB/OB*, C57BL/6 mice wild-type for the *leptin* gene; *ob/ob*, leptin-deficient mice; Control, no T0901317 treatment. Significant differences from *OB/OB* or *ob/ob* mice with Control: \* $P < 0.05$ , \*\* $P < 0.01$ , \*\*\* $P < 0.001$ .

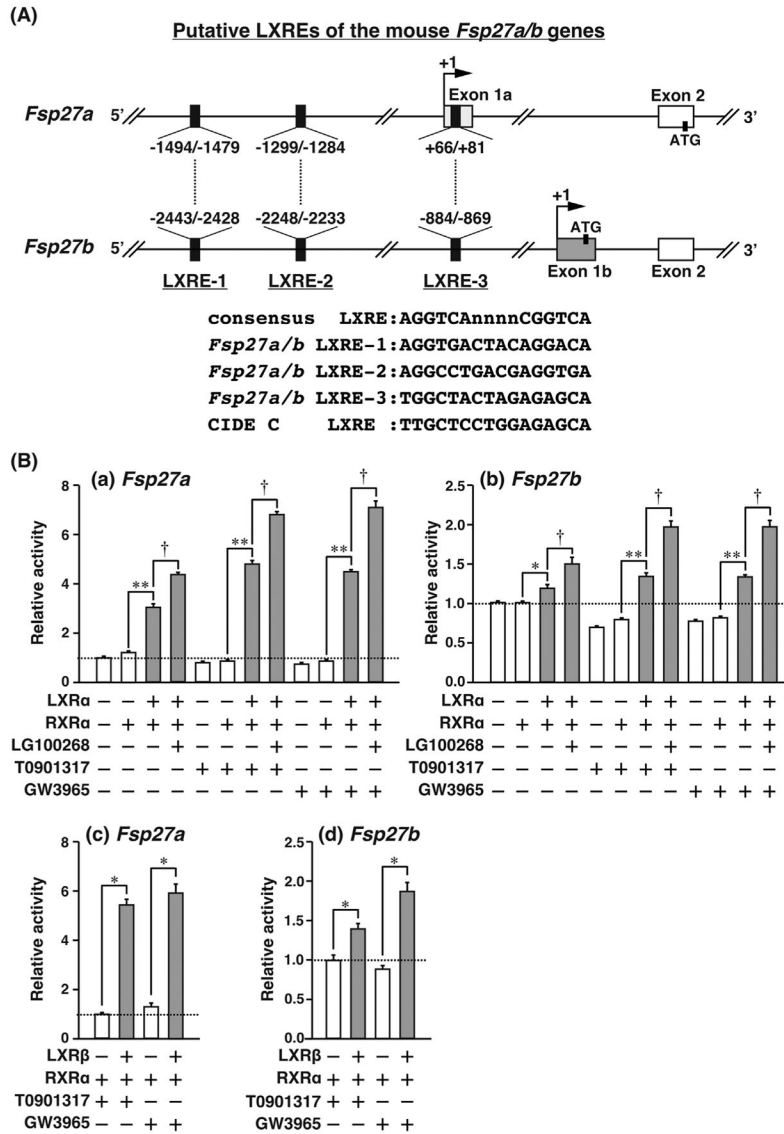


**Fig. 2. LXRα promotes the promoter activity of *Fsp27a* and *Fsp27b*.**  
 (A) Location and sequences of three putative LXREs in the 5'-region or exon 1 of mouse *Fsp27a* and *Fsp27b* genes. Arrow and ATG indicate transcription and translation start sites, respectively. (B) *Fsp27a* A1 including -1698/+257 region (a) and *Fsp27b* B1 including -2647/+77 region (b) reporter plasmids were transfected into HEK293FT cells with or without the expression plasmids for LXRα. *Fsp27a* A1 (c) and *Fsp27b* B1 (d) reporter plasmids were transfected into HEK293FT cells with or without the expression plasmids for LXRβ. Six hours after transfection, the medium was changed to fresh medium containing 10 μM T0901317, 10 μM GW3965, or 0.1 μM LG100268. The cells were harvested at 42 h after transfection and luciferase activity was measured. Each bar represents the average ± S.E.M. of three individual experiments. Significant differences from cells without LXRα or LXRβ expression plasmid: \**P* < 0.01, \*\**P* < 0.001. Significant differences from cells without LG100268: † *P* < 0.001.

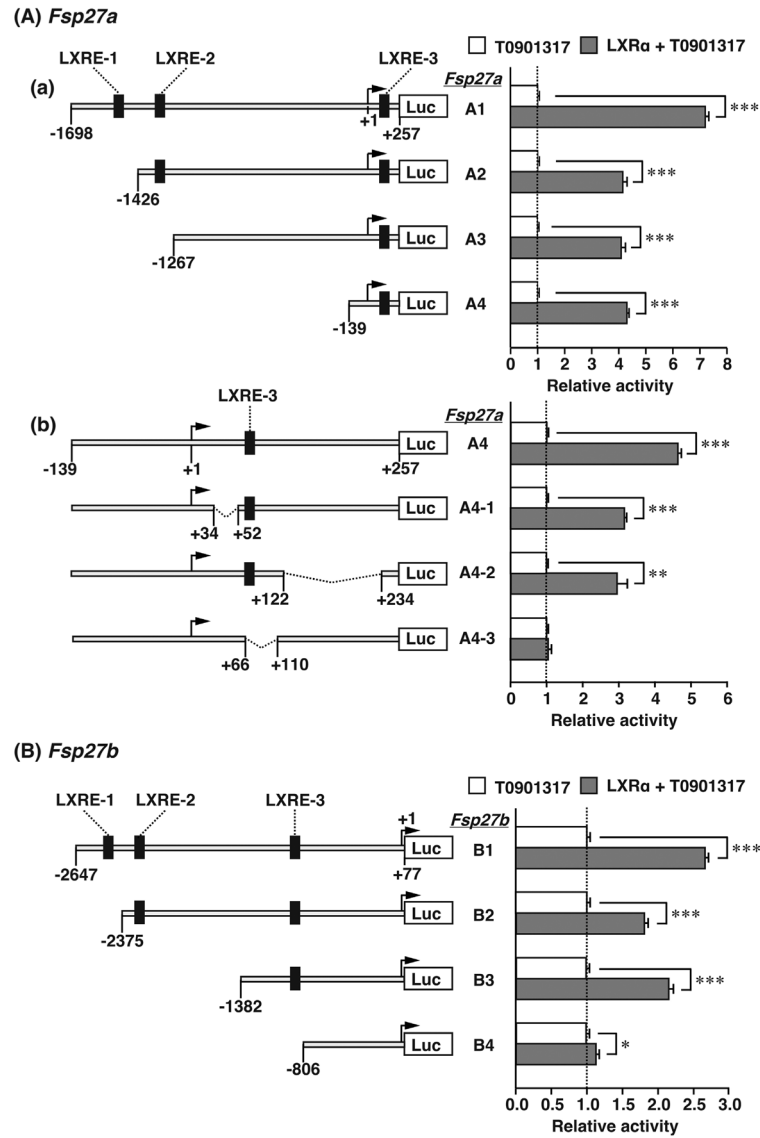


**Fig. 3. Induction of the promoter activity of *Fsp27a* and *Fsp27b* genes by T0901317 depends on two LXREs.**

(A) (a) Serially deleted *Fsp27a* A1–A4 and (b) internally deleted *Fsp27a* A4-1–A4-3 reporter plasmids were transfected into HEK293FT cells with or without LXR $\alpha$  expression plasmid. (B) Serially deleted *Fsp27b* B1–B4 reporter plasmids were transfected into HEK293FT cells with or without LXR $\alpha$  expression plasmid. In (A) and (B), 6 h after transfection, the medium was changed to fresh medium containing 10  $\mu$ M T0901317. The cells were harvested at 42 h after transfection and luciferase activity was measured. Each bar represents the average  $\pm$  S.E.M. of three individual experiments. Significant differences from cells without LXR $\alpha$  expression plasmid: \* $P$  < 0.01, \*\* $P$  < 0.001.

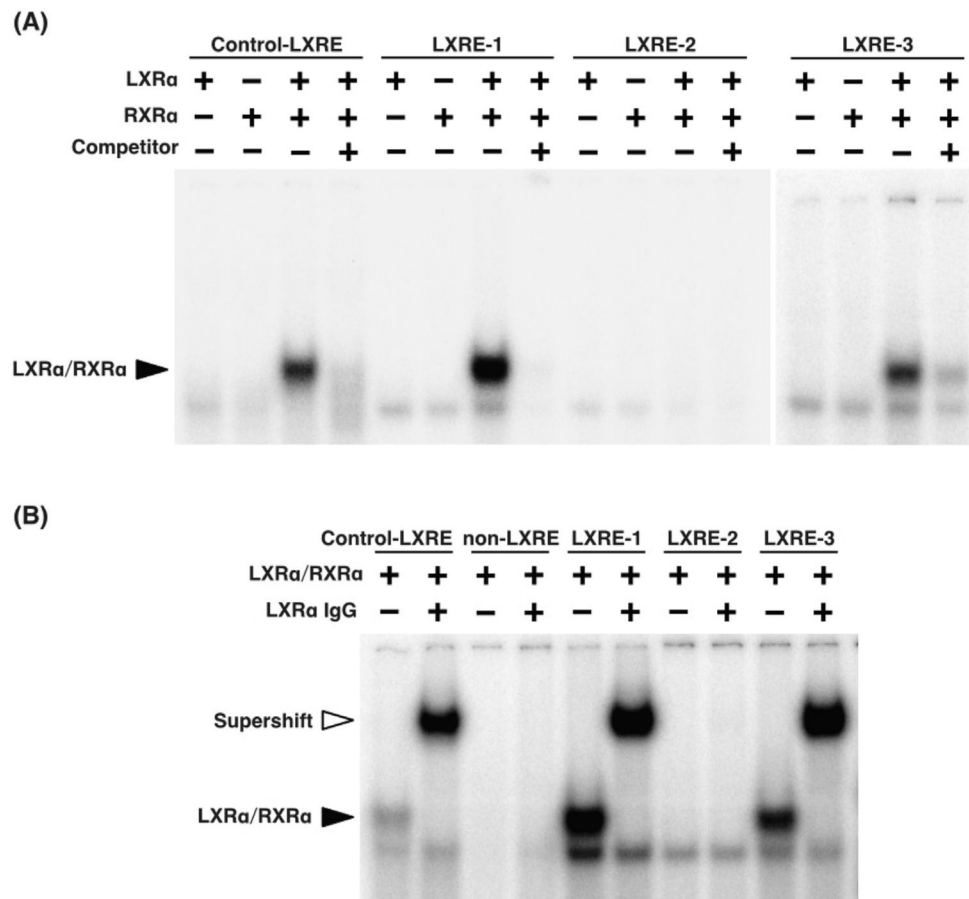


**Fig. 4. LXR $\alpha$ /RXR $\alpha$  heterodimers directly bind to LXRE-1 and LXRE-3 in the *Fsp27a/b* 5'-upstream or 5'-UTR region.**

(A) EMSAs were performed using  $^{32}$ P-labeled oligonucleotide probes. Probes were incubated with LXR $\alpha$ /RXR $\alpha$  produced by *in vitro* translation with or without an excess of unlabeled probe as competitor. (B) Supershift assays were performed using anti-LXR $\alpha$  IgG. The location of the LXR $\alpha$ /RXR $\alpha$  complex is indicated by the filled arrowhead, while the supershifted complex is indicated by the open arrowhead.



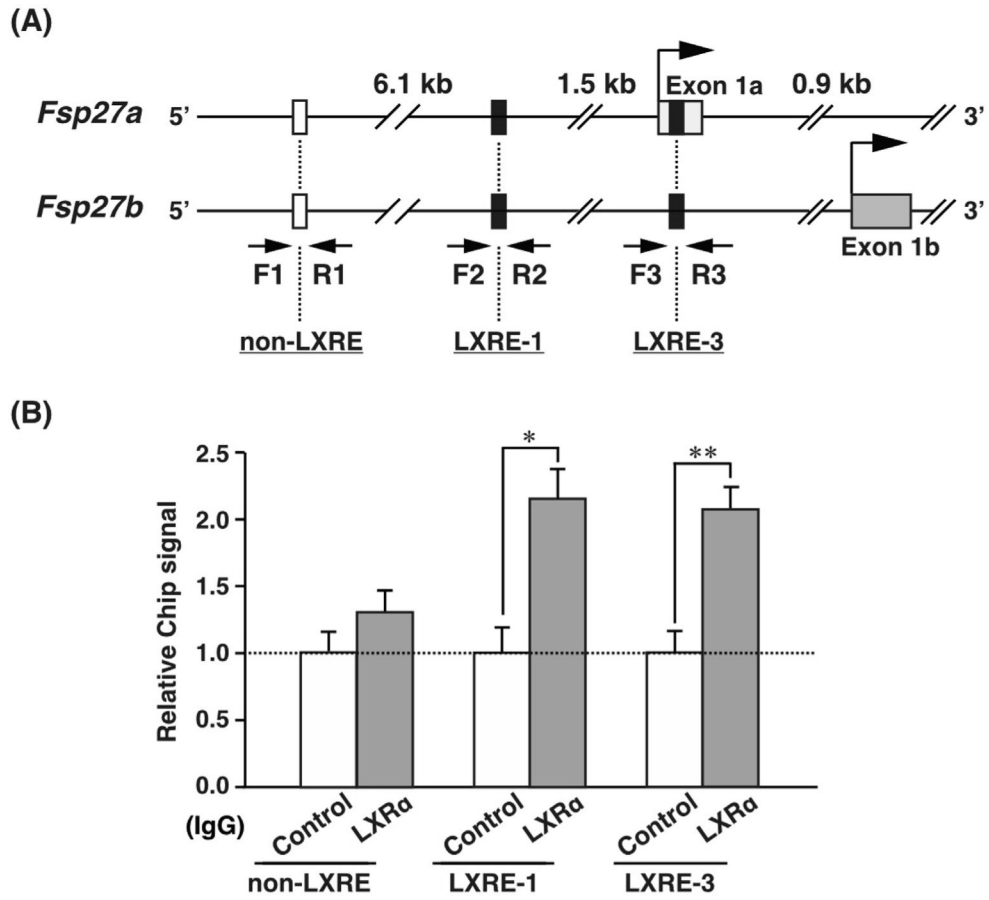


**Fig. 5. Endogenous LXR $\alpha$  associates with LXRE-1 and LXRE-3.** (A) The positions of ChIP primer pairs are shown by arrows. F1 and R1 primer sets located >6.1 kb upstream of *Fsp27a/b* were also used as negative controls. (B) ChIP-qPCR analysis was performed using chromatin samples from the livers of T0901317-treated *ob/ob* mouse liver with anti-rabbit IgG (control) or anti-LXR $\alpha$  IgG. Each bar represents the average  $\pm$  S.E.M. of three individual experiments. Significant differences from Control: \* $P$  < 0.01, \*\* $P$  < 0.001.